ICAS 2021 SHANGHAI
International Council of the Aeronautical Sciences
32nd Congress of the International Council of the Aeronautical Sciences
September 6-10, 2021 Pudong Shangri-La, Shanghai, China

METHODICAL STUDIES OF THE POSSIBILITY TO APPLY A NUMERICAL METHOD WITH BUILD-IN EMPIRICAL CRITERIA FOR DETERMIMING THE LAMINAR-TO-TURBULENT TRANSITION ON THE CONE SURFACE AT HIGH MACH NUMBERS

Voevodenko N.V.[1], Shvalev Yu.G.[1]

[1] Central Aerohydrodynamic Institute named after Professor N.E. Zhukovsky (TsAGI), 1 Zhukovsky Street, Zhukovsky Moscow Region, 140180 Russian Federation

Abstract

This work is a methodological fundamental study of the possibility to use empirical criteria and formulas built into the numerical method to determine the laminar-turbulent transition (LTT) in the boundary layer on the surface of streamlined bodies. A methodology is described for calculating the flow around slender bodies at high speeds, based on the solution of the Euler equations, in which empirical criteria for the LTT determining are embedded. The developed methodology is approximate and is intended for fast engineering calculations of flows with LTT on complex surfaces. The results of studies of the position and shape of LTT on the surface of a cone using a numerical method with built-in empirical criteria of Simeonides and Berry are presented.

Keywords: fundamental research, numerical methods, laminar-turbulent transition, empirical criteria

1. Introduction

At high supersonic flight speeds, a significant effect on the aerodynamic characteristics of an aircraft (AC) is exerted by the phenomenon of a laminar-turbulent transition (LTT) in the boundary layer (BL) on its surface. First of all, LTT affects the thermal processes, aerodynamic drag and aerodynamic quality of the aircraft. Numerical modeling of LTT is a very difficult problem even for the current level of development of computer technology and numerical methods.

The LTT phenomenon is very complex and diverse, and its position and character depend on a number of factors, such as the pressure gradient, the degree of freestream turbulence, and many others. Moreover, depending on these factors, not only the LTT position changes, but also the transition scenario determined by the development of disturbances in the boundary layer. In a number of problems, the position and nature of the LTT have a significant impact on the solution as a whole. In this case, the high accuracy of the aerodynamic coefficients calculating, in particular, the coefficients of lift and drag, is impossible without taking into account and correctly describing of LTT. Recently, many different approaches to the LTT modeling have been developed. Within the framework of the so-called differential transition models, the transport equations are solved, which make it possible to determine the position and nature of the transition, in combination with equations for the characteristics of turbulence (k, ε, ω). These models are relatively easy to integrate into modern computational codes and can be used to solve arbitrary problems. As stated above, the LTT nature significantly depends on various external factors, such as:

- the degree of freestream turbulence;
- direction and magnitude of the pressure or temperature gradient;
- the presence of roughness or blowing / suction on the surface, etc.

Depending on the combination of these factors, the following types of LTT are usually distinguished:

1. Natural transition. It is observed in problems of external aerodynamics with low levels of freestream turbulence. At present, it is generally believed that if its degree of turbulence is below 1%, the laminar BL becomes linearly unstable when the local Re number exceeds the critical value, after which Tollmien – Schlichting (TS) disturbances (waves) arise. These disturbances grow downstream, turning into longitudinal and transverse vortices, and then

into turbulent spots - the so-called Emmons spots. They increase in size and gradually fill the entire BL. A well-known schematic representation of the natural LTT process proposed by G. Schlichting [1] is shown in Figure 1.

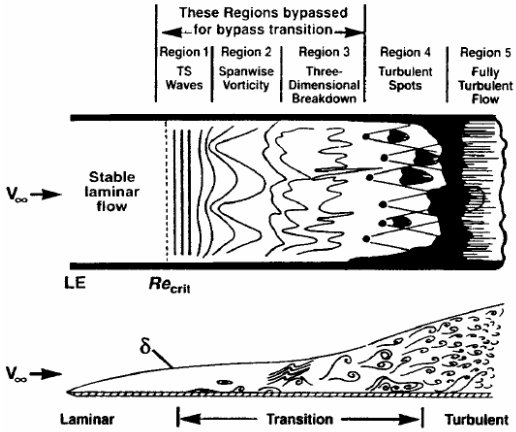

Figure 1 - Scheme of natural LTT [1]

2. Forced or "bypass" transfer (from the English bypass - to pass, bypass). At turbulence levels in the flow external to the BL above 1%, the first and, possibly, the second and third stages of the natural transient process (Fig. 1) are bypassed, and turbulent spots arise directly under the influence of external disturbances. With this type of transition, strong turbulent pulsations from the free flow penetrate into the BL, leading to its rapid turbulence. This scenario was named “bypass” because during its implementation the stage of appearance and development of TS waves is “skipped”. It is clear that the boundary between the "bypass" and natural transitions is not strictly defined in terms of the level of turbulence. A bypass transition can also occur due to the roughness of the streamlined surface, rather than due to turbulence in the external flow, or when the turbulent flow is directly injected into BL.

3. Detachable (bubble) transition. This type of transition is observed in flows with a strong positive pressure gradient downstream. In this separation scenario of the transition, the laminar BL is detached from the surface, which leads to rapid turbulization of the shear layer. In addition, a turbulent BL can relaminarize, for example, under the influence of a strong favorable pressure gradient.

4. Transition due to cross-flow instability (so-called "cross-flow" transition). This type of transition is fundamentally three-dimensional and is found, for example, on the wings of aircraft. The transition to turbulence occurs due to the instability of the transverse component of the velocity in the boundary layer, which arises as a result of the presence of an inflection in the velocity profile. For example, on a wing with a large sweep, a three-dimensional BL develops, which has a significant lateral velocity component. This is commonly referred to as transverse flux, which can lead to inflectional instability of the BL and to the transition much earlier than it would be in the case of a pure growth of TS waves. Currently, two types of transverse disturbances are distinguished: stationary and wandering. It is believed that the stationary transverse instability is excited by the surface roughness, and a nonstationary source is required for the appearance of the wandering transverse instability, for example, a gradual increase in the freestream turbulence. On a swept wing, all three sources of disturbances (i.e., TS waves, stationary and wandering transverse instabilities) are present and can interact with each other if they become large enough.

It is of fundamental importance that when the above-mentioned parameters change, not only the position and intensity of the transition, but also its type can change. In fact, on complex surfaces of real aircraft, transitions of different types take place, they mix and mutually affect each other. However, in practice, in most cases we are dealing with natural and bypass transfers. Therefore, in this work, the main attention is paid to these two types of LTT.

In the range of high supersonic speeds, the LTT phenomenon has its own characteristic features (see, for example, [2]). The problematical character of validation of the LTT numerical simulation is noted. Unfortunately, most ground test data are not reliable enough due to operation in traditional

noisy wind tunnels (WT) and shock tubes with disturbance levels much higher than in flight. Transition mechanisms operating in low disturbance environments can be altered or completely bypassed in high flow disturbance environments.

However, the studies carried out at TsAGI showed that with Mach number increase, the effect of the free-stream turbulence level decreases rapidly and, starting from M = 5, becomes generally insignificant.

Flight tests do not have problems with WT flow disturbances and should form the final basis for evaluating LTT calculation methods. But flight tests also have their limitations associated with both the physics of the phenomenon and a very high cost.

Correct LTT numerical simulation seems to be possible on the basis of direct numerical simulation of the Navier-Stokes equations (DNS - methods). However, nowadays even supercomputers can simulate 3D non-stationary DNS solutions only for fairly simple geometries, such as a plate or an inclined plane. The construction of DNS solutions for bodies of complex geometry close to real aircraft is technically impossible, since it requires the amount of computations and computer resources that are orders of magnitude higher than those available to modern computers.

In connection with the complexity of the phenomenon under consideration, along with numerical modeling, empirical methods are being developed that predict the onset of LTT and its length using simple formulas. They were derived as a result of generalization and analysis of large arrays of experimental data obtained both in the wind tunnel and in the flight experiment. However, empirical methods also have significant limitations and require methodological studies for validation, determining the range of their applicability and accuracy.

Therefore, in this work, for the study of LTT, an engineering technique is proposed, in which the empirical criteria of LTT are implemented into a numerical method for solving the Euler equations. The position and shape of the LTT on the cone surface in a wide range of M, Re numbers and angles of attack have been investigated. The calculation results are compared with the data of experimental studies of the LTT in the TsAGI T-116 high-speed wind tunnel.

2. Numerical method and empirical formulas and criteria

2.1 Method for calculating the local parameters Re_δ and M_δ on the BL outer boundary

The basis of this method for modeling high-speed flow around bodies is the numerical solution of the Euler equations. This solution can be obtained using the NINA software package [3-4] or using any other package that implements the numerical solution of the Euler equations. As a result of the numerical solution (NINA package), we obtain the values of the inviscid flow parameters at the centers of the cells adjacent to the body surface, as shown in Figure 2. We take the values of the parameters in the cells adjacent to the body surface as the values of the parameters at the BL external surface. We get the following parameters:

$$\frac{p}{\rho_\infty U_\infty^2};\frac{\rho}{\rho_\infty};\frac{u}{U_\infty};\frac{v}{U_\infty};\frac{w}{U_\infty}.$$

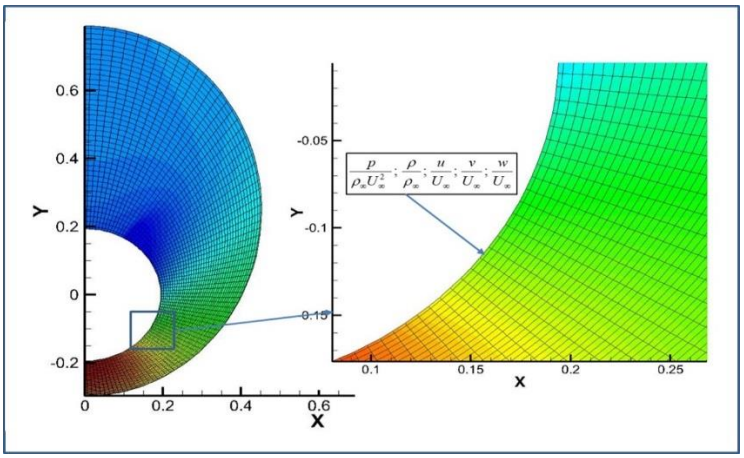

Figure 2 - Determination of parameters at the BL external surface.

The index δ denotes the value of the parameter at the BL external surface and we assume:

$$p_\delta = \frac{p}{p_\infty}; \rho_\delta = \frac{\rho}{\rho_\infty}; u_\delta = \frac{u}{U_\infty}; v_\delta = \frac{v}{U_\infty}; w_\delta = \frac{w}{U_\infty}$$

To calculate the Re value of the LTT onset - the critical number Re_{tr}, the Re and M numbers are required at the external surface of the boundary layer - Re_δ and M_δ. The value of M_δ is given by the following relations:

$$\mathrm{M}_\delta = \frac{\sqrt{u^2 + v^2 + w^2}}{a}; \quad a = \sqrt{\gamma \frac{p}{\rho}}$$

After substitution of dimensionless quantities, we get:

$$\mathrm{M}_\delta = \sqrt{\frac{(u_\delta^2 + v_\delta^2 + w_\delta^2)U_\infty^2}{(\gamma p_\delta p_\infty)/(\rho_\delta \rho_\infty)}} = \sqrt{\frac{(u_\delta^2 + v_\delta^2 + w_\delta^2)}{p_\delta / \rho_\delta} \frac{U_\infty^2}{(\gamma p_\infty)/(\rho_\infty)}} = \mathrm{M}_\infty \sqrt{\frac{u_\delta^2 + v_\delta^2 + w_\delta^2}{p_\delta / \rho_\delta}}$$

To calculate the local number Re_δ, we use the following relations:

$$\mathrm{Re}_\delta = \mathrm{Re}_{1\text{м}} \frac{\rho_\delta u_\delta x}{\mu_\delta}; \quad \mathrm{Re}_{1\text{м}} = \frac{\rho_\infty u_\infty}{\mu_\infty},$$

$$\frac{p}{\rho} = RT; \quad T_\delta = \frac{T}{T_\infty} = \frac{p/p_\infty}{\rho/\rho_\infty} = \frac{p_\delta}{\rho_\delta}; \quad \mu_\delta = \frac{\mu}{\mu_\infty} = f\left(\frac{T}{T_\infty}\right) = f(T_\delta),$$

where $Re_{1м}$ is the number Re of the freestream flow per 1m.

Local length x is defined as the distance from the cone nose to the center of the cell. The dynamic viscosity coefficient μ depends only on temperature and can be calculated either by the Sutherland formula or using a power-law formula, which is also widely used in practice.

2.2 Simeonides and Berry Criteria

Having obtained the values of Re_δ and M_δ, we can calculate the local values of the critical Reynolds number Re_{tr} using empirical criteria. In this work, for this purpose, the criteria of Simeonides [5-6] and Berry [7-8] were applied. The Simeonides criterion was obtained in the European Space Agency (ESA). As a result of the analysis and generalization of a large amount of test data in different wind tunnel and flight, obtained in different countries and organizations, an empirical formula was derived to determine Re_{tr} [5] on the surface of the cone:

$$Re_{tr} = 5 \cdot 10^5 \cdot M_\delta^{0.8} \cdot {Re_b}^{0.1},$$

where Re_b is the local Reynolds number calculated from the bluntness radius of the cone.

The length of the transition region $Re_{\Delta x}$ is also determined using the empirical formula obtained by Simeonides for a plate [6]:

$$Re_{\Delta x} = (60 + 4.86 \cdot M_\delta^{1.92}) \cdot {Re_{tr}}^{2/3}$$

The second criterion used in this work was obtained at NASA and was widely used in the NASP and X-43A projects to determine the LTT. It determines the correlation between the Reynolds number calculated from the thickness of the momentum loss Re_θ with the local Mach number at the boundary of the BL M_δ:

$$Re_\theta / M_\delta \geq 300 \div 450.$$

Thus, to apply the Berry criterion, it is necessary to know the local value of the pulse loss thickness δ **. To calculate δ **, we use the Blasius formula [9], which is an exact solution of the equations of a laminar PS for an incompressible fluid flow around a plate at a zero pressure gradient. To calculate δ ** in a compressible fluid, we use Young's approximate empirical formula [10], which is sufficient and convenient in practical applications. The indicated formulas for calculating δ ** were obtained for a plate. To determine Re_θ of the beginning of LTT on the cone, we use the fact that the thickness of the momentum loss on the cone at the same values of x in √3 is less than on the

plate. This follows from the solution of the equations for a laminar BL on a cone [11]:

$$Re_{\theta tr\_co} = 300 \cdot \sqrt{3} \cdot M_{\delta}\text{, так как } \delta^{**}_{cone} = \frac{\delta^{**}_{plane}}{\sqrt{3}}$$

The LTT length will be determined by the Simeonides formula, since the Berry criterion does not give the length of the transition region.

2.3 Methodology of the local Stanton number and the drag coefficient calculation

The ultimate goal of this work is to create an engineering technique for calculating the local drag coefficient taking into account the LTT and an efficient and fast numerical method for calculating the aerodynamic characteristics of high-speed aircraft using this technique.

When calculating the local drag coefficient, we use the Reynolds analogy [12], which establishes a simple relationship between friction and heat transfer and allows one to obtain an equation for determining the local drag coefficient. This relationship is determined by the ratio:

$$c_f = 2S \cdot St_{\delta},$$

where St_{δ} is the local Stanton number, the value of S depends on the Prandtl number, but in engineering practice, a sufficiently good accuracy is given by S = 0.825 in a turbulent BL and S = 0.8 in a laminar BL.

To calculate the local Stanton number - St_{δ} and the friction drag coefficient - c_f for laminar and turbulent BL, we use the empirical formulas of Yu.G. Shvalev and N.F. Ragulin [13-14]. These formulas were obtained on the basis of numerous experimental studies in the TsAGI's T-116 wind tunnel.

To calculate the local values of St_{δ} and c_f in each cell of the mesh adjacent to the body surface, we use the following algorithm:

- if the local Reynolds number $Re_{\delta} < Re_{tr}$, we take the values of the local Stanton number and the drag coefficient equal to the corresponding values for the laminar BL [13],

- if $Re_{\delta} > Re_{tr} + Re_{\Delta x}$, we take the values of the local Stanton number and the drag coefficient equal to the corresponding values for a turbulent BL [14],

- if $Re_{tr} < Re_{\delta} < Re_{tr} + Re_{\Delta x}$, the local Stanton number and the drag coefficient are determined by linear interpolation.

3. Calculation results

3.1 Changing the LTT position on the cone when changing the M number and angle of attack

The method described above for calculating flows with LTT was applied to calculate the flow around a cone with a half-angle at the apex Θ = 10° in the range of Mach numbers from 2 to 10. The results obtained using the Berry and Simeonides criteria are compared. Figure 3 shows the picture of the laminar-turbulent transition obtained according to the Berry criterion on the surface of the cone with Θ = 10° at M = 3, the angle of attack α = 10° and the Reynolds number of the freestream flow to 1m equal to $7.66 \cdot 10^6$.

In Figure 3, the green area is the laminar flow BL area, the purple area is the turbulent flow BL area, and the blurred area around the white stripe represents the LTT zone. The transition region is essentially three-dimensional and in shape resembles a section of a cone by a plane at an angle to its axis. With an increase in the freestream Mach number, the section plane seems to shift downstream.

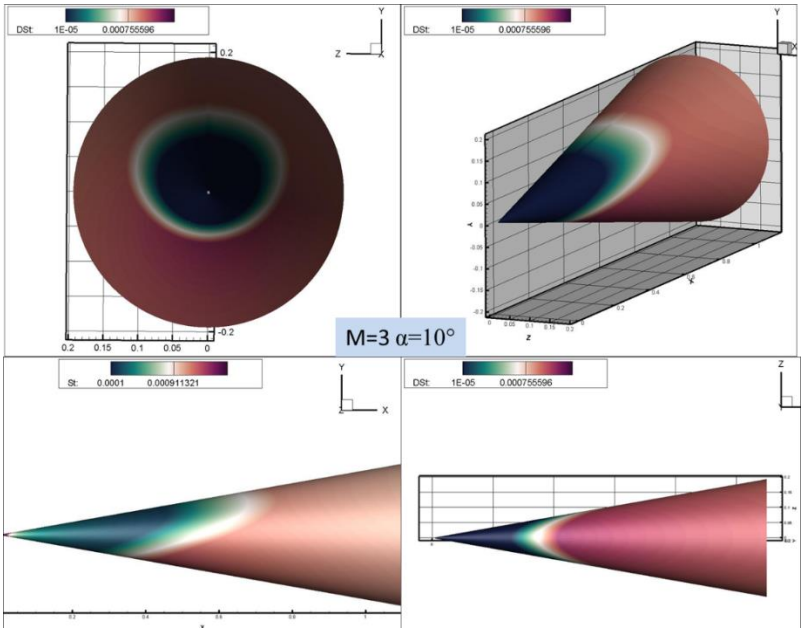

Figure 3 - LTT pattern on a cone with a semi-angle at the apex Θ = 10 ° at M = 3 and α = 10 °.

Figure 4 groups the results of calculations using various LTT criteria at M = 3 ÷ 10, angle of attack α = 10° and the Reynolds number of the freestream flow to 1m equal to $7.66 \cdot 10^6$. The first thing that draws attention to itself is how qualitatively similar are the LTT pictures obtained using completely different criteria of Simeonides and Berry, as well as with Re_{tr} = const (the const values were chosen $Re_{tr} = 3.5 \cdot 10^6$ with M = 3 and 4, $Re_{tr} = 4.5 \cdot 10^6$ at M = 5, $Re_{tr} = 5 \cdot 10^6$ at M = 7 and 10). In this case, the values of Re_{tr} themselves, of course, differ, but the overall LTT picture remains very similar when different criteria are applied.

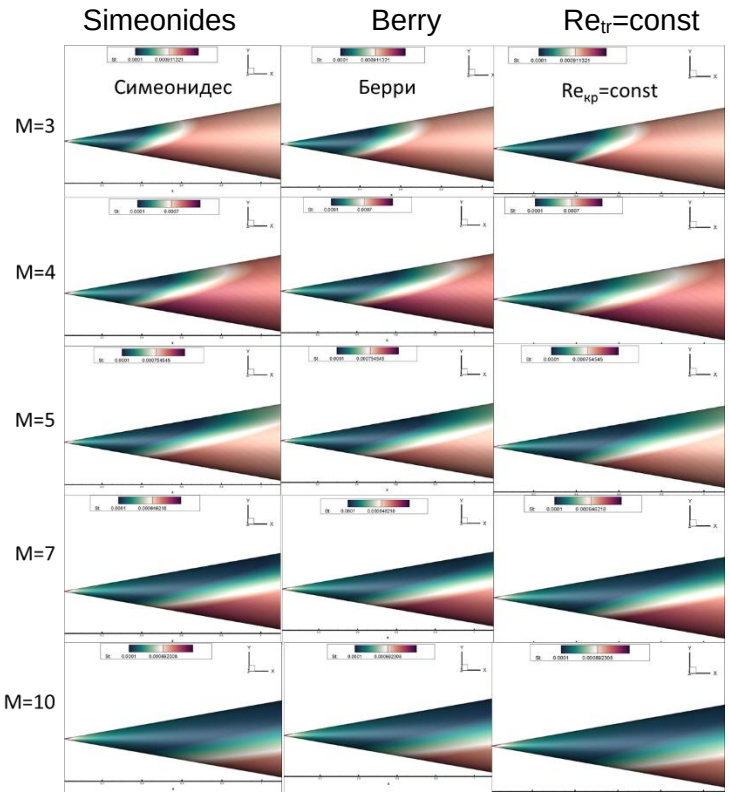

Figure 4 - LTT pattern on a cone with a semi-angle at the apex Θ = 10° at M = 3 ÷ 10 and α = 10°.

The change in the shape and position of the LTT with an increase in the M number at an angle of attack α = 10° is shown in Figure 5. Here are the results of calculations using the Berry criterion, the Simeonides criterion gives similar results. As can be seen, at M = 2, the flow in the boundary

layer is mainly turbulent (purple area), and only in a small area near the nose is laminar flow (green area). With an increase in the Mach number, the LTT shifts downstream, and at M = 10, most of the surface is flown around with a laminar BL. In this case, the LTT region on the leeward side shifts much faster than on the windward side, and already starting from M = 5, the LTT region goes beyond the cone boundary, and the flow becomes completely laminar. At the same time, a zone of transitional and turbulent flows remains on the windward side.

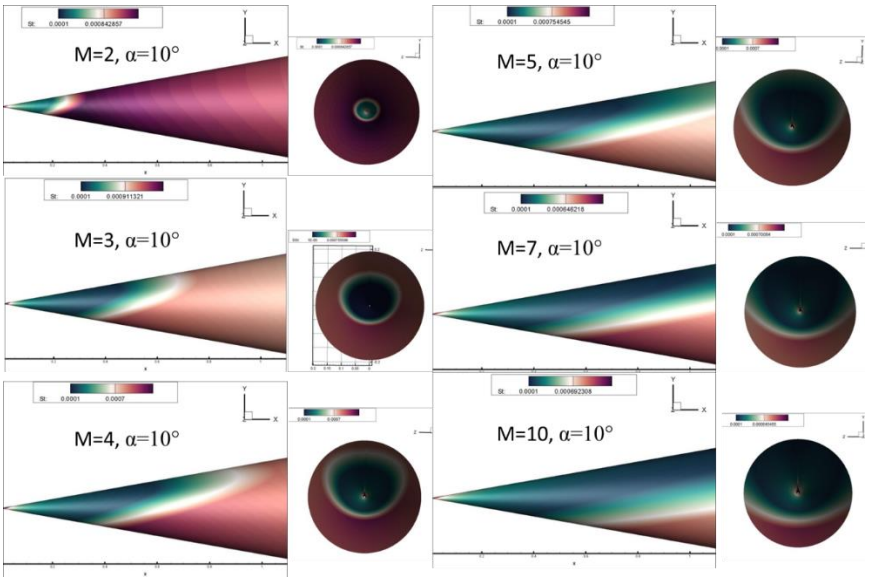

Figure 5 - LTT on a cone at M = 2 ÷ 10, α = 10°, Berry's criterion.

The presented results show that with an increase in the angle of attack, the LTT on the windward side shifts upstream relative to its position at α = 0, and on the leeward side - downstream. This tendency is consistent with the classical results given in the book [11] (§120, p. 715), where the experimental dependence of Re_{tr} on M_∞ for the plate (Figure 6) is shown and an important fact is noted that the LTT shifts upstream to M_∞ = 3.5, and downstream with further growth of M_∞. The velocity on the external boundary of the BL on a cone at an angle of attack grows from bottom to top; therefore, LTT first appears on below, then on the side, and then on above. It is this tendency characteristic of large M numbers that is reflected in the criteria of Simeonides and Berry.

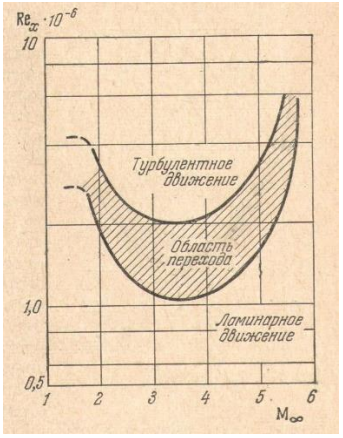

Figure 6 - LTT on a plate, drawing from the book [11] (§120, p. 715).

Numerous studies of the transition pattern on the cone in T-116 show that first LTT occurs on the windward side of the cone, downstream on the lateral surface, and then on the leeward side. In particular, this was noted in [15].

When flowing around a cone at a zero angle of attack, we are dealing with a fairly simple conical flow, and the position of the LTT depends only on the numbers M and Re and the distance from the nose. When flowing around a cone at an angle of attack, the flow in the boundary layer becomes substantially three-dimensional and much more complex. Therefore, the LTT zone is displaced and deformed. The change in the shape of the LTT zone with an increase in the angle of

attack α from zero to 30° at M = 3, Re1m = 7.66 · 106 is shown on the left in Figure 7. In these calculations, the Simeonides criterion was used. It can be seen from the presented pictures that, on the windward side of the cone, with an increase in the angle of attack α, the LTT zone slightly shifts upstream, but this shift is insignificant. At the same time, on the leeward side, with an increase in α, the LTT quickly shifts downstream and, at α = 20°, goes beyond the cone boundary. This behavior of the LTT zone is in full agreement with the experimental data [15].

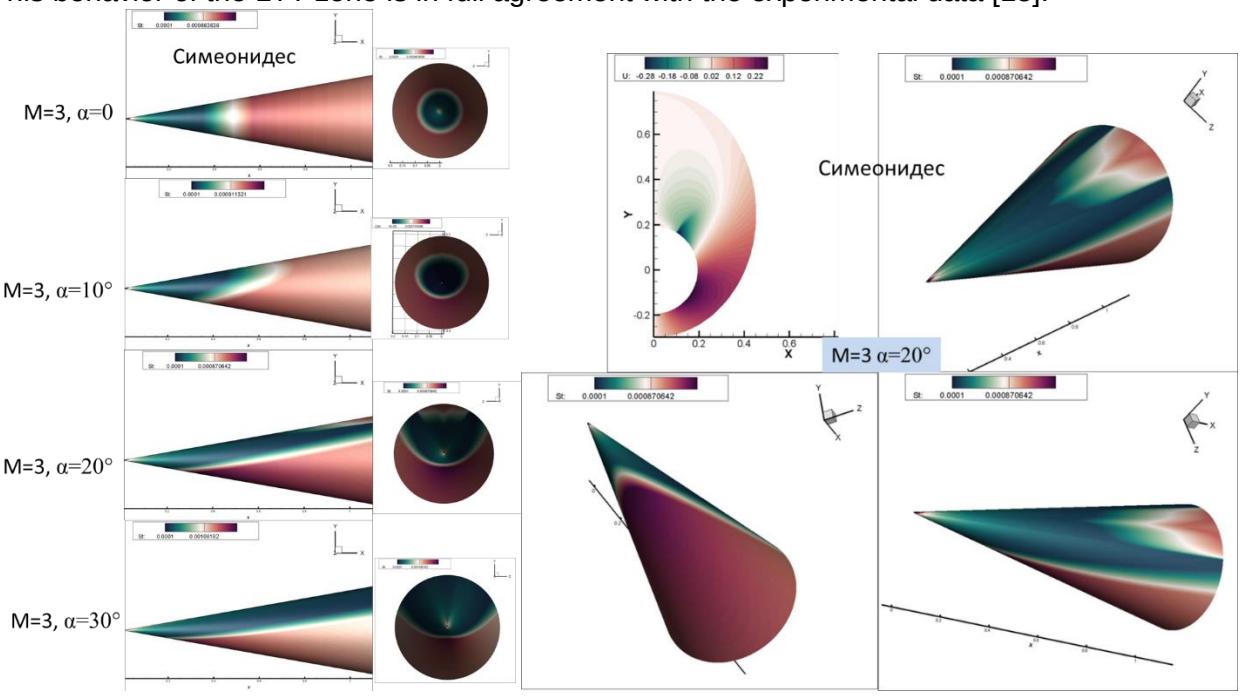

Figure 7 - LTT on a cone at M = 3 and α = 0 ÷ 30°.

It is also interesting to note one more feature of the phenomenon under consideration. LTT on a cone is basically of the natural transition type 1, described in Introduction. With an increase in the angle of attack on the leeward side of the cone, vortices arise, which, falling on the surface of the cone, cause the so-called forced or bypass transition type 2. Here, turbulent spots arise in the boundary layer directly under the influence of disturbances in the external flow. With this type of transition, strong turbulent pulsations from the external flow penetrate into the BL, leading to its rapid turbulence. In the center of Figure 7, a cross-section of the velocity field is shown, and the vortex is clearly visible. And on the right, you can see the areas of the bypass transition caused by this vortex on the leeward side of the cone. With a further increase in the angle of attack, the vortices move upward, and at α = 30° the described phenomenon is no longer observed. Such a picture of the LTT qualitatively corresponds to the physical structure of the flow on the leeward side of the cone, obtained in experimental studies and described in [15].

3.2 Comparison of calculation results with experiment

Comparison of the calculation results with the experimental data obtained in the high-speed wind tunnel TsAGI T-116 [15] shows that the data of both criteria and experiment are quite close. As an example, Figure 8 on the left shows the distributions of the Stanton number - St on the surface of the cone at M = 7, α = 20 °, obtained numerically using the Simeonides criterion and in experiment. The arrows in the pictures indicate: the total length of the cone in the experiment, equal to 0.55m, and the beginning of the LTT on the lower generatrix x≈0.295m. The graphs on the right show comparisons of the distributions of the Stanton number along the lower, lateral and upper generatrices of the cone. The numerical method based on empirical criteria, in this case, gives a result very close to the experiment.

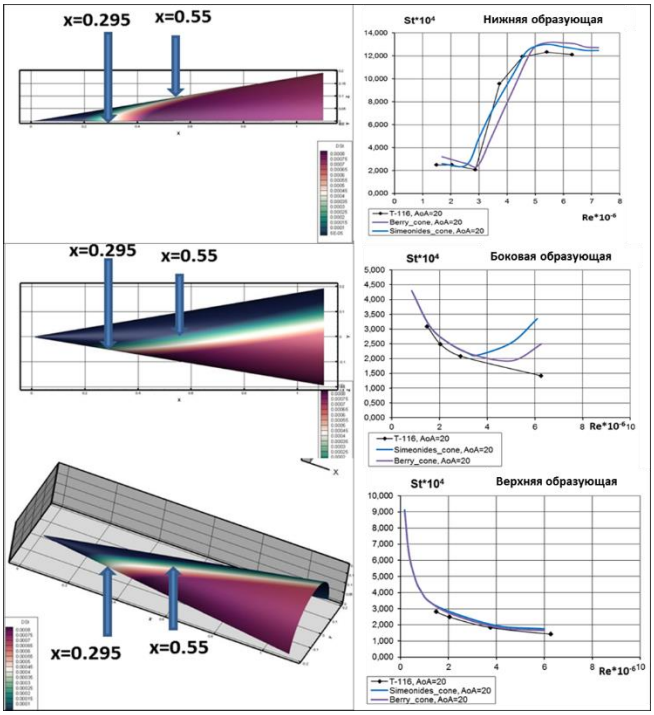

Figure 8 - Test of empirical criteria: transition on a taper at M = 7, α = 20°, $Re_{1M} = 11.4 \cdot 10^6$.

Figure 9 shows the curves of the beginning and end of the LTT zone depending on the Mach number on a cone with a half angle at the apex Θ = 10° at α = 0. The freestream Reynolds number to 1_M $Re_{1M} = 7.66 \cdot 10^6$ for all numbers M. Figure 10 shows the influence of the freestream Reynolds number on the beginning and end of the LTT at M = 4. The presented graphs show that, in general, freestream Re_{1M} has little effect on the critical Reynolds number.

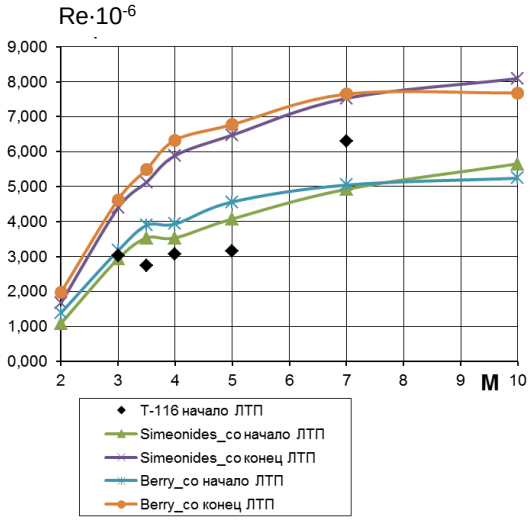

Figure 9 - The beginning and end of the LTT zone depending on the Mach number on a cone with a semi-angle at the apex Θ = 10° at α = 0.

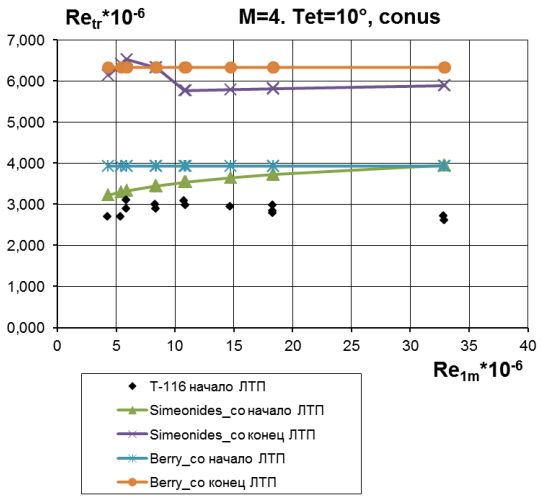

Figure 10 - Influence of Re_{1M} on the onset and end of the LTT zone on a cone with a semi-angle at the apex Θ = 10° at M = 4 and α = 0.

4. Conclusion

Methodological studies of the possibility of using the numerical-empirical method, which incorporate the criteria of Simeonides and Berry for assessing the beginning and length of the LTT region, and empirical formulas for calculating the local values of the Stanton number and the drag coefficient have been carried out. The laminar-turbulent transition on the cone surface is investigated in a wide range of M, Re numbers and angles of attack with different empirical criteria and a comparison with the data of experimental studies at TsAGI T-116 wind turbine, which has shown qualitative agreement.

The LTT zone on the surface of the cone at an angle of attack has a complex three-dimensional shape. With an increase in the number M, the LTT zone shifts downstream, and at M = 7 and 10, most of the surface is flown around with a laminar BL, and, on the leeward side, the LTT region shifts much faster than on the windward one. With an increase in the angle of attack at a fixed M number on the leeward side, the LTT also rapidly shifts downstream and, at α = 20°, goes beyond the cone boundary.

Basically, a natural LTT arises on the surface of the cone; however, at moderate angles of attack (α = 20°), a bypass transition appears to arise on the leeward side, caused by vortices arising on the surface of the cone.

In general, the flow around the cone, starting from M = 3, is mixed laminar-turbulent; therefore, in the considered flow regimes, it is necessary to use computational methods with modeling the LTT.

5. Contact Author Email Address

Contact author - Nina Voevodenko, TsAGI, whose Email адрес - nina.voevodenko@tsagi.ru

6. Copyright Statement

References

[1] Шлихтинг Г. *Теория пограничного слоя*. Пер. с нем. под ред. Л.Г. Лойцянского. – М.: Наука, 1974.

[2] Башкин В.А., Егоров И.В. *Численное исследование задач внешней и внутренней аэродинамики.* – М: ФИЗМАТЛИТ, 2013. Smith J, Jones B and Brown J. The title of the conference paper. *Proc Conference title*, where it took place, Vol. 1, paper number, pp 1-11, 2001.

[3] Воеводенко Н.В. Возможности расчета обтекания летательных аппаратов сложных форм при больших сверхзвуковых числах Маха с использованием гиперзвуковой теории малых

возмущений. *Журнал «Ученые записки ЦАГИ»*, 1988, том XIX, № 6.

[4] Voevodenko N.V. Computation of Supersonic/Hypersonic Flow Near Complex Configurations. *19th International Congress of the Aeronautical Sciences*, Anahime, CA, USA, ICAS-94-5.2.3, 1994.

[5] Simeonides G. A. and Kosmatopoulos E., Laminar-Turbulent Transition Correlation in Supersonic/Hypersonic Flow. *25th International Congress of the Aeronautical Sciences*, Hamburg, Germany, 2006.

[6] Simeonides G. A., Laminar-Turbulent Transition Correlations in Supersonic/Hypersonic Flat Plate Flow. *24th International Congress of the Aeronautical Sciences*, Yokohama, Japan, 2004.

[7] Berry S., Di Fulvio M. and Kowalkowski K. Forced Boundary Layer Transition on X-43 (Hyper-X) in NASA LaRC 20-Inch Mach 6 Air Tunnel. *NASA/TM*-2000-210316, 2000.

[8] Berry S. et al., Boundary Layer Transition on X-43A. *38th AIAA Fluid Dynamics Conference*, Seattle WA, USA, AIAA-2008-3736, 2008.

[9] Blasius H., Grenzschichten in Flüssigkeiten mit kleiner Reibung, *Zeitschr. of Math. U. Phys*. 56, 1908.

[10] Юнг. А. «Пограничные слои», статья в сборнике *«Современное состояние аэродинамики больших скоростей»* под редакцией Л. Хоуорта, т. I, ИЛ, Москва, 433, 1955.

[11] Лойцянский Л.Г. *Механика жидкости и газа*. Изд. 5, переработанное, Главная редакция физико-математической литературы издательства «Наука», Москва, 1978.

[12] Reynolds O. On the extent and action of the heating surface for the steam boilers. *Proceed. of the Manchester Literary and Philosophical Society* 14, 1874.

[13] Швалев Ю.Г. Экспериментальное исследование местной теплоотдачи в ламинарном пограничном слое при сверхзвуковых скоростях. *Журнал «Ученые записки ЦАГИ»*, Т. IX, № 5, 1978.

[14] Рагулин Н.Ф., Швалев Ю.Г. Экспериментальное исследование местной теплоотдачи в турбулентном пограничном слое при сверхзвуковых скоростях. *Инженерно-физический журнал*, Т. XLV, №4, 1983.

[15] Швалев Ю.Г. Исследования перехода ламинарного пограничного слоя в турбулентный на моделях в аэродинамической трубе Т-116 ЦАГИ. *Журнал «Труды ЦАГИ»*, Выпуск 2693, 2011.